Force and Diffusion Measurements in Sub-Doppler Laser Cooling

M. D. Hoogerland, H. F. P. de Bie, H. C. W. Beijerinck, and K. A. H. van Leeuwen
Physics Department, Eindhoven University of Technology, P.O. Box 513, 5600 MB Eindhoven, The Netherlands

P. van der Straten
Debye Institute, Rijksuniversiteit Utrecht, P.O. Box 80000, 3508TA Utrecht, The Netherlands

E. J. D. Vredenbregt and H. J. Metcalf
Physics Department, State University of New York at Stony Brook, Stony Brook, New York 11794
(Received 25 June 1993)

We present the first direct measurements of the velocity dependence of the average force and diffusion constant for metastable neon atoms in a one-dimensional $\sigma^+\sigma^-$ laser cooling configuration. Force and diffusion are determined, respectively, from the deflection and broadening of a highly collimated atomic beam by its interaction with a pair of counter-running laser beams. The interaction time is much shorter than the characteristic damping time of the cooling process. The resulted force and diffusion measurements are compared with the results of both semiclassical and quantum Monte Carlo calculations.

PACS numbers: 32.80.Pj, 42.50.Vk

Laser cooling to temperatures below the Doppler limit has been studied extensively, both in experiments and in theory. Experiments have been performed on a variety of configurations leading to sub-Doppler cooling, among which are polarization gradient cooling with linear ($\pi^x\pi^y$) [1–3] and circular polarization ($\sigma^+\sigma^-$) [3], magnetically induced laser cooling (MILC) [4,5], velocity-selective magnetic resonance cooling [5–7], cooling by Raman resonances [8], adiabatic cooling in an intense standing wave [9], and velocity-selective coherent population trapping [10]. In all these cases, the velocity distribution is measured after an interaction time much longer than the damping time of the cooling process. The most extensive data on the final velocity distribution as a function of laser detuning and intensity in both $\sigma^+\sigma^-$ and $\pi^x\pi^y$ configurations have been obtained by Weiss *et al.* [3] in an experiment studying laser cooling in one dimension.

Several theoretical models have been proposed which allow the calculation of sub-Doppler laser cooling forces [11–18]. These include both semiclassical and quantum mechanical (distinguished by the quantization of the center-of-mass motion) approaches. The models are based on either a density matrix formalism or a quantum Monte Carlo simulation. Results of actual calculations of the force are given, e.g., by Ungar *et al.* [12] and by Nienhuis *et al.* [13].

Thus far, no direct experimental determination of the velocity dependence of the force and diffusion in a sub-Doppler cooling configuration has been published. In this work we present such measurements for the first time. A collimated atomic beam of metastable neon atoms is intersected by a near-resonant light field formed by two counter-running laser beams with orthogonal circular polarization ($\sigma^+\sigma^-$ configuration). We chose this $\sigma^+\sigma^-$ polarization gradient configuration because the light shifts do not depend on position and dipole forces do not play a role. By contrast, for the $\pi^x\pi^y$ configuration, spatially periodic dipole forces do exist and lead to "channeling" phenomena that complicate the analysis of experimental results.

The initial value of the transverse velocity $v_\perp$ of the atoms (i.e., the component of the velocity along the $\mathbf{k}$ vectors of the light) can be varied. The interaction time, determined by the size of the laser beams and the axial velocity of the atoms, is so short that the change in $v_\perp$ due to the forces exerted by the light on the atoms is small compared to the initial value of $v_\perp$. The final transverse velocity distribution is measured. From the average change in $v_\perp$, the average force exerted on the atoms during the interaction time is determined; from the broadening of the initially narrow distribution, the average diffusion coefficient is determined. The results are compared with semiclassical calculations based on the work of Nienhuis *et al.* [13] as well as quantum Monte Carlo calculations according to the method proposed by Dum *et al.* [15]. The agreement is excellent.

In our experiment the atomic beam is produced in a supersonic expansion. The neon atoms are excited to the metastable $\{3s\,^3P_2\}$ state in a dc discharge. The average axial velocity of the atoms in the beam is 1200 ms^{-1}, and the rms velocity spread is 250 ms^{-1}. Immediately after the nozzle, the effective source area is restricted by a 50 × 500 μm vertical slit. An identical slit, positioned 2 m downstream, collimates the atomic beam to an rms angular spread of 10 μrad. With the 1200 ms^{-1} average axial velocity, this angular spread corresponds to a transverse velocity spread of 0.012 ms^{-1}, small compared to the single-photon recoil velocity for neon of 0.031 ms^{-1}.

After the second slit, the atomic beam interacts with an elliptical Gaussian standing laser wave with a waist radius ($1/e^2$ intensity) of 0.6 mm in the direction of the atomic beam axis and 3.1 mm across the beam's 500 μm

0031-9007/94/72(21)/3332(4)$06.00

height. The CW dye laser light is tuned near resonance with the two-level transition to the $\{3p\,^3D_3\}$ level at $\lambda = 640.225$ nm. The saturated absorption signal from a Zeeman-tuned gas discharge cell is used to control the precise tuning of the laser to within 1 MHz. The Earth's magnetic field in the interaction region is canceled using a full set of Helmholtz coils.

The angle between atomic and laser beams, and therefore the initial transverse velocity of the atomic beam with respect to the laser beam $v_\perp$, can be changed by moving the collimating slit. The atomic transverse velocity distribution after the interaction is probed by scanning a channeltron detector with a 50×2000 μm entrance slit, 1.75 m downstream of the interaction region, across the beam profile. The atomic beam is chopped to allow time-of-flight analysis of the axial velocity of the detected metastable atoms. Thus slit and detector positions can be unambiguously translated into transverse velocities. Transverse velocity distributions are measured with and without laser beams; from these data, the change in average velocity and the increase in its variance are determined.

In order to define a time-averaged force and momentum diffusion constant, the effective length of the interaction region is defined by the width of an "equivalent square profile" with the same rms spread and same integrated area (total laser power) as the Gaussian laser beam profile. The width of this equivalent profile divided by the average axial velocity determines the effective interaction time.

In Fig. 1 the measured $v_\perp$ dependence of the averaged force and diffusion constant is shown for a laser detuning $\Delta = -2\Gamma$ with $\Gamma = 5.15 \times 10^7$ rad/s the natural linewidth of the transition (natural lifetime $\tau = 19.4$ ns), and a laser intensity per laser beam (at the center of the Gaussian) of $150\,\mathrm{W/m^2}$. This intensity corresponds to a saturation parameter $s = I/I_{\mathrm{sat}} = 3.8$ for each beam with $I_{\mathrm{sat}} = 2\pi hc/6\tau\lambda^3$. Force and diffusion are given in units of $\hbar k\Gamma/2$ and $\hbar^2k^2\Gamma/4$, respectively.

The various theoretical results are also shown in Fig. 1. The dashed line represents the steady-state force on an atom whose velocity is held constant ("drag force"), calculated using the semiclassical operator description of Nienhuis *et al.* [13]. For this calculation, the effective laser intensity is determined by the height of the equivalent square profile. The experimentally observed force is a factor of 3–4 lower than the steady-state drag force. This is caused by the transient effect discussed by Ungar *et al.* [12]: the interaction time is short compared to the time needed for the ground state populations and coherences to reach the steady-state values.

The dotted lines correspond to the results of a time-dependent calculation using Nienhuis' semiclassical formalism. In this calculation, the traversal of the atom through the Gaussian laser beam is represented by taking the laser intensity to vary in time with a Gaussian envelope. The rms width of this Gaussian profile is 0.27

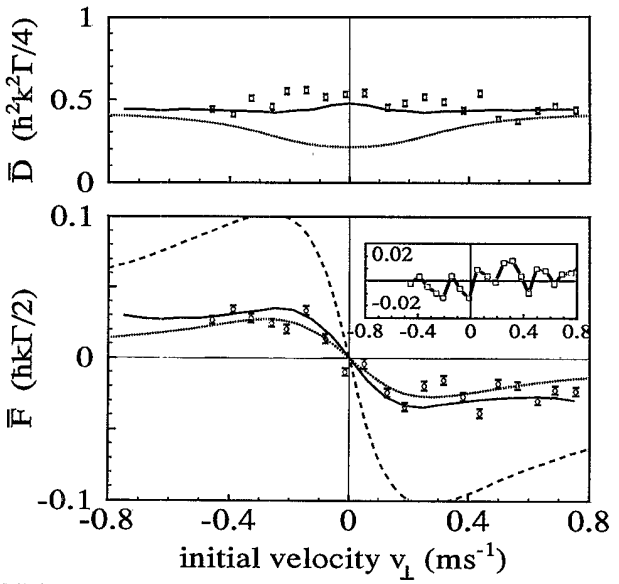

FIG. 1. The averaged force (lower frame) and diffusion (upper frame) as a function of initial velocity $v_\perp$ for a detuning of $\Delta = -2\Gamma$ and a maximum laser intensity of 150 W/m^2 ($s = 3.8$). The force and diffusion are given in units of $\hbar k\Gamma/2$ (equal to the maximum radiation pressure force) and $\hbar^2k^2\Gamma/4$ (the maximum diffusion in a purely one-dimensional two-level system), respectively. The semiclassical (dotted line) and quantum Monte Carlo (full line) calculations are shown as well. The dashed line represents the semiclassical steady-state "drag force." In the inset in the lower frame, the difference between experimental and quantum Monte Carlo results is shown in the same units as in the outer frame.

μs or 14τ. As the axial velocity of the atoms is large and does not change appreciably during the interaction with the light, this representation is justified. Individual atom trajectories are followed by integrating the evolution of the density matrix for a number of initial positions of the atom in the light wave, and for all initial lower level substates. From the density matrix the force on an atom is determined from Eq. (8.3) of Ref. [13], and the atomic position and transverse velocity are adjusted accordingly. For each individual semiclassical atomic trajectory, the diffusion is calculated from Eqs. (6.2) and (61.12) from Ref. [13]. The diffusion determines the width of the probability distribution for the final transverse velocity, which is assumed to be Gaussian. The total final velocity distribution is calculated by adding the contributions from the individual trajectories. From the average change in $v_\perp$, and from the variance in the distribution, the averaged force and diffusion coefficients are determined in the same way as for the experimental data.

The full lines correspond to a quantum mechanical calculation following the Monte Carlo approach of Dum *et al.* [15]. An incoming atom is represented by a plane atomic wave, propagating in the direction of the laser beams, with the atom in a randomly chosen lower level substate. The coherent evolution of the wave function

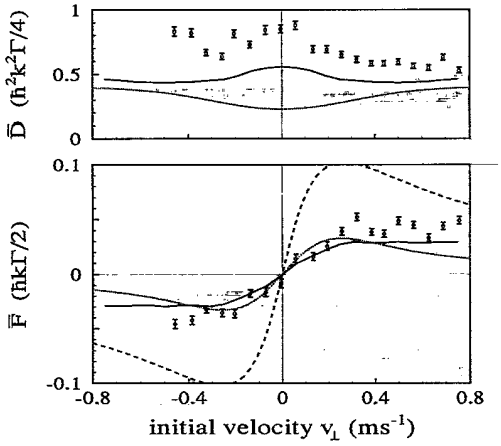

FIG. 2. The averaged force (lower curves) and diffusion (upper curves) as a function of initial velocity $v_\perp$ for a detuning of $\Delta = 2\Gamma$ and a maximum laser intensity of 144 W/m^2 ($s = 3.6$). The semiclassical (dotted line) and quantum Monte Carlo (full line) calculations are shown as well. The dashed line represents the semiclassical steady-state "drag force."

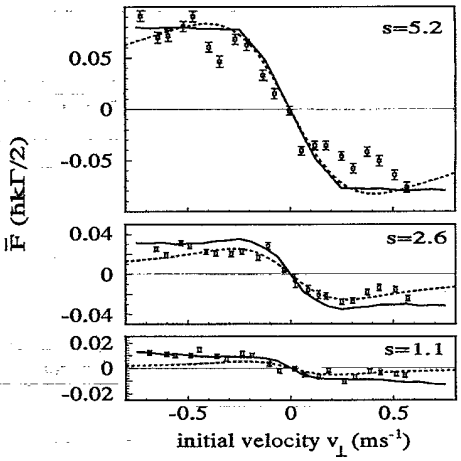

FIG. 3. The force as a function of initial velocity $v_\perp$ for three laser intensities. The semiclassical (dotted line) and quantum Monte Carlo (full line) calculations are shown as well. In all curves the detuning $\Delta = -1.6\Gamma$.

(between spontaneous emissions) is calculated on a basis consisting of the products of the internal atomic substates and the family of one-dimensional center-of-mass momentum states with momentum $p = p_0 + 2n\hbar k$ for the lower level substates and $p = p_0 + (2n+1)\hbar k$ for the upper level substates, respectively, with $\mathbf{p}_0$ the initial momentum, n an integer number, and k the photon wave number. The time to the next spontaneous emission is generated stochastically according to the loss of total probability of the coherent wave function. At a spontaneous emission event, the branching ratios for the polarization of the spontaneous decay are calculated first. The polarization of the emitted photon is then randomly determined using these ratios. The recoil of the photon is taken into account by changing p_0 with the appropriate amount for the recoil direction, randomly chosen according to the correct angular distribution for the chosen polarization. The internal wave function is then projected to the ground state sublevels and renormalized, retaining the associated upper-state center-of-mass wave functions. The total interaction time is taken to start and end at the $1/e^4$ points of the Gaussian intensity profile. The final momentum distribution is averaged over 2000 Monte Carlo realizations, from which average deflection and momentum spread, and hence averaged force and diffusion constants are determined.

The agreement for the averaged force calculated from Nienhuis' semiclassical formalism is very good, as can be seen in Fig. 1. However, the dip in the averaged diffusion predicted by this semiclassical theory and by earlier quantum calculations (see, e.g., Castin and Mølmer [19]), is not reproduced in the experiment. The agreement between quantum Monte Carlo (QMC) calculations and experiment in Fig. 1 is excellent, both for the force and for the diffusion. The deviation between semiclassical and QMC calculations for the force at higher initial velocities is caused by the fact that the semiclassical calculation does not include the Doppler cooling force. It is interesting that, contrary to the semiclassical results, the QMC results predict a slight increase in diffusion at $v_\perp = 0$. The experimental accuracy, however, is not high enough to confirm the existence of the predicted small increase.

In Fig. 2 results for positive detuning are shown. The expected reversal of the curve is evident in both experiment and calculations, although the agreement for the positive detuning data is not as good as for negative detuning.

Figures 3 and 4 display the force and diffusion coefficients, respectively, for a fixed detuning $\Delta = -1.6\Gamma$ and different laser intensities, corresponding to $s = 1.1$, 2.6, and 5.2, respectively. Again, the agreement between

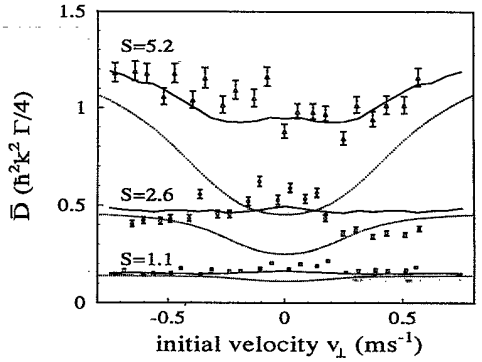

FIG. 4. The diffusion constant as a function of initial velocity $v_\perp$ for three laser intensities. The semiclassical (dotted line) and quantum Monte Carlo (full line) calculations are shown as well. In all curves the detuning $\Delta = -1.6\Gamma$.

experiment and both calculations is quite good for the force, while the QMC calculation reproduces the diffusion data as well. The differences between the QMC and the semiclassical force curves at higher $v_\perp$ are again due to the exclusion of the Doppler force.

The deviations between theory and experiment for all force-vs-velocity curves are nevertheless larger than the errors indicated, which correspond to the (1σ) statistical errors resulting from the data analysis. Closer inspection shows that the deviations are systematic and appear as an oscillation with a period of ≈ 0.22 ms^{-1}. This is illustrated by the inset in Fig. 1, where the difference between experimental and QMC results for the force is shown. It has been checked by examining other data sets that the deviations are reproducible. The oscillation period is fixed. So far, we have found no explanation for this effect.

In this work we have demonstrated that the velocity dependence of the average force and diffusion in one-dimensional $\sigma^+\sigma^-$ polarization gradient cooling can be experimentally determined by studying the deflection and broadening of a well-collimated atomic beam. Quantum Monte Carlo and semiclassical calculations are in excellent agreement with the experimentally determined force; the former calculation reproduces the diffusion data as well. The results show that, as the atomic density matrix is still evolving towards the steady state, the measured force is much smaller than the steady-state "drag force." In a future experiment, the interaction time will be varied to study the dynamics of the cooling process explicitly.

This work is financially supported by the Dutch Foundation for Fundamental Research on Matter (FOM), the Dutch Royal Academy of Sciences (KNAW), NSF, and ONR.

[1] P. Lett, R. Watts, C. Westbrook, W. D. Phillips, P. Gould, and H. Metcalf, Phys. Rev. Lett. **61**, 169 (1988).
[2] Y. Shevy, D. S. Weiss, P. J. Ungar, and S. Chu, Phys. Rev. Lett. **62**, 1118 (1989).
[3] D. S. Weiss, E. Riis, Y. Shevy, P. J. Ungar, and S. Chu, J. Opt. Soc. Am. B **6**, 2072 (1989).
[4] B. Sheehy, S-Q. Shang, P. van der Straten, and H. J. Metcalf, Phys. Rev. Lett. **64**, 858 (1990).
[5] M. D. Hoogerland, H. C. W. Beijerinck, K. A. H. van Leeuwen, P. van der Straten, and H.J. Metcalf, Europhys. Lett. **19**, 669 (1992).
[6] S-Q. Shang, B. Sheehy, P. van der Straten, and H. J. Metcalf, Phys. Rev. Lett. **65**, 317 (1990).
[7] S-Q. Shang, B. Sheehy, H. J. Metcalf, P. van der Straten, and G. Nienhuis, Phys. Rev. Lett. **67**, 1094 (1991).
[8] M. Kasevich and S. Chu, Phys. Rev. Lett. **69**, 1741 (1992).
[9] J. Chen, J. G. Story, J. J. Story, and R. G. Hulet, Phys. Rev. Lett. **69**, 1344 (1992).
[10] A. Aspect, E. Arimondo, R. Kaiser, N. Vansteenkiste, and C. Cohen-Tannoudji, Phys. Rev. Lett. **61**, 826 (1988).
[11] J. Dalibard and C. Cohen-Tannoudji, J. Opt. Soc. Am. B **6**, 2023 (1989).
[12] P. J. Ungar, D. S. Weiss, E. Riis, and S. Chu, J. Opt. Soc. Am. B **6**, 2058 (1989).
[13] G. Nienhuis, P. van der Straten, and S-Q. Shang, Phys. Rev. A **44**, 462 (1991).
[14] J. Dalibard, Y. Castin, and K. Mølmer, Phys. Rev. Lett. **68**, 580 (1992).
[15] R. Dum, P. Zoller, and H. Ritsch, Phys. Rev. A **45**, 4879 (1992).
[16] A. M. Steane, G. Hillenbrand, and C. J. Foot, J. Phys. B **25**, 4721 (1992).
[17] S. M. Yoo and J. Javanainen, Phys. Rev. A **45**, 3071 (1992).
[18] T. Bergeman, Phys. Rev. A **48**, R3425 (1993).
[19] Y. Castin and K. Mølmer, J. Phys. B **23**, 4101 (1990).